Journal of Statistical Physics, Vol. 34, Nos. 5/6, 1984

Phase Transitions in Diluted Magnets: Critical Behavior, Percolation, and Random Fields

R. J. Birgeneau,[1] R. A. Cowley,[2] G. Shirane,[3] and H. Yoshizawa[3]

Received September 30, 1983

Transition metal halides provide realizations of Ising, XY, and Heisenberg antiferromagnets in one, two, and three dimensions. The interactions, which are of short range, are generally well understood. By dilution with nonmagnetic species such as Zn^{++} or Mg^{++} one is able to prepare site-random alloys which correspond to random systems of particular interest in statistical mechanics. By mixing two magnetic ions such as Fe^{++} and Co^{++} one can produce magnetic crystals with competing interactions—either in the form of competing anisotropies or competing ferromagnetic and antiferromagnetic interactions. In this paper the results of a series of neutron scattering experiments on these systems carried out at Brookhaven over the past several years are briefly reviewed. First the critical behavior in $Rb_2Mn_{0.5}Ni_{0.5}F_4$ and $Fe_cZn_{1-c}F_2$ which correspond to two-dimensional and three-dimensional random Ising systems, respectively, are discussed. Percolation phenomena have been studied in $Rb_2Mn_cMg_{1-c}F_4$, $Rb_2Co_cMg_{1-c}F_4$, $KMn_cZ_{1-c}F_3$, and $Mn_cZn_{1-c}F_2$ which correspond to two- and three-dimensional Heisenberg and Ising models, respectively. In these cases c is chosen to be in the neighborhood of the nearest-neighbor percolation concentration. Application of a uniform field to the above systems generates a random staggered magnetic field; this has facilitated a systematic study of the random field problem. As we shall discuss in detail, a variety of novel, unexpected phenomena have been observed.

KEY WORDS: Critical phenomena; neutron scattering; random interactions; antiferromagnets; percolation and random fields.

[1] Department of Physics, Massachusetts Institute of Technology, Cambridge, Massachusetts 02139.
[2] Department of Physics, University of Edinburgh, Edinburgh EH9 3JZ, Scotland.
[3] Brookhaven National Laboratory, Upton, New York 11973.

0022-4715/84/0300-0817$03.50/0

1. INTRODUCTION

It has been recognized in the past few years that quenched randomness may cause a fundamental change in the phase transition behavior of solid state systems. For small randomness in the interactions the effects are quite subtle; however, if impurities generate even quite small random fields then the phase transition is destroyed in both two and three dimensions. For systems with large randomness, especially with competing interactions, entirely new phenomena may occur. These include percolation effects, spin glass, and reentrant spin glass behavior.

In studies of critical phenomena in pure systems, experiments on "model" compounds have played an essential role. It is not surprising therefore, that experiments on simple systems with well-characterized, easily controllable randomness are playing an important role in elucidating critical phenomena in the presence of quenched randomness. The fluorides and chlorides of the three-dimensional (3D) transition metals turn out to be ideal systems in which to study the properties of disordered systems. Transition metal ions such as Mn^{++}, Co^{++}, Fe^{++}, and Mg^{++} are chemically very similar but magnetically very different. Consequently, it is possible to grow single crystals in which the magnetically very different ions are distributed at random over the transition metal sites so that the systems are chemically quite uniform but magnetically very different. Fortunately it has also turned out, for the fluorides at least, that it is possible to grow single-crystal alloys which are of very high quality crystallographically. This greatly facilitates optical, transport, and especially, scattering measurements.

We have carried out a series of neutron scattering experiments on mixed magnetic crystals over the past several years. In this paper we review the salient results of these measurements. Emphasis will be on our studies of *diluted* magnetic insulators such as $Rb_2Co_cMg_{1-c}F_4$. In these crystals one can address the issues of random exchange critical behavior, percolation, and random field effects. We should emphasize that in this paper we intend primarily to review the results of experiments by the authors and their collaborators at Brookhaven; no attempt is made to survey comprehensively the entire field.

The general phase diagram together with random exchange critical behavior are discussed in Section 2. Percolation phenomena are presented in Section 3. In Section 4 we review experiments to date on the random field problem.

2. RANDOM ISING CRITICAL BEHAVIOR

The phase diagram for diluted two-dimensional (2D) square lattice antiferromagnets with nearest-neighbor (nn) interactions[1] is shown sche-

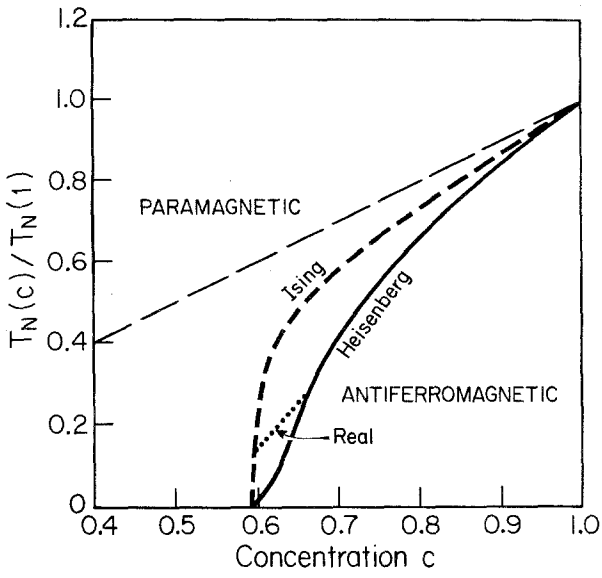

Fig. 1. Schematic phase diagram of a diluted 2D square-lattice antiferromagnet with nearest-neighbor interactions. The Heisenberg system is assumed to have an infinitessimal 3D interaction in order to produce a phase transition to conventional long-range order. The "real" curve corresponds to a 2D Heisenberg model with about 1% dipolar Ising anisotropy. Figure from Ref. 6.

matically in Fig. 1. In the pure system, $c = 1$, one expects an ordinary 2D phase transition. This has, for example, been well explored in the systems K_2CoF_4 and Rb_2CoF_4, which are realizations of the 2D Ising model[2] Remarkably good agreement is found with Onsager's exact results. There is also a large variety of materials such as K_2NiF_4 and Rb_2MnF_4 which have predominantly Heisenberg interactions but with a small Ising anistropy. Gratifyingly, these also show 2D Ising critical behavior.[3] These systems may be readily diluted with the nonmagnetic isomorphs K_2MgF_4 or Rb_2MgF_4. With increasing dilution T_c decreases rapidly until for $c = c_p = 0.594$ the phase transition vanishes; c_p is the site percolation concentration for the nn square lattice problem.[4] The explicit shape of the phase boundary near c_p depends both on the percolation crossover exponent ϕ and on the temperature variable relevant to the system Hamiltonian—T for models with continuous symmetry and $e^{-2J/kT}$ for Ising models.

For $c_p < c < 1$ one expects to observe *random exchange* critical behavior; in this section we concentrate on this aspect of the problem. The first experiments on random Ising critical behavior were not carried out on a diluted system but rather in the mixed alloy $Rb_2Mn_{0.5}Ni_{0.5}F_4$.[3] In that

system the Hamiltonian may be written

$$\mathscr{H} = \sum_{\substack{\langle ij \rangle \\ i,jNN}} J_{ij}\mathbf{S}_i \cdot \mathbf{S}_j + \sum_i g_i \mu_B H_i^A S_i^Z \tag{1}$$

with $J_{\text{Mn-Mn}} = 7.4$ K, $J_{\text{Mn-Ni}} = 25.7$ K, and $J_{\text{Ni-Ni}} = 89$ K; here $S(\text{Mn}) = 5/2$ and $S(\text{Ni}) = 1$. The mean reduced anisotropy field, which arises from a combination of crystal field and dipolar interactions, is

$$h_i = \left\langle g_i \mu_B H_i^A \cdot \left(\sum_{j=\text{nn}} J_{ij} S_j \right)^{-1} \right\rangle = 0.0071 \tag{2}$$

From neutron scattering experiments one can readily measure the correlation length and susceptibility above T_N and the order parameter below T_N. Results for the correlation lengths in the pure and mixed systems are shown in Fig. 2. As predicted by theory, all three show 2D Ising critical behavior. Any possible logarithmic corrections[7] due to the randomness in $Rb_2Mn_{0.5}Ni_{0.5}F_4$ are too small to be observed. Similar agreement is found for the susceptibility and order parameter.

More recently, Ikeda[8] has studied the critical behavior in

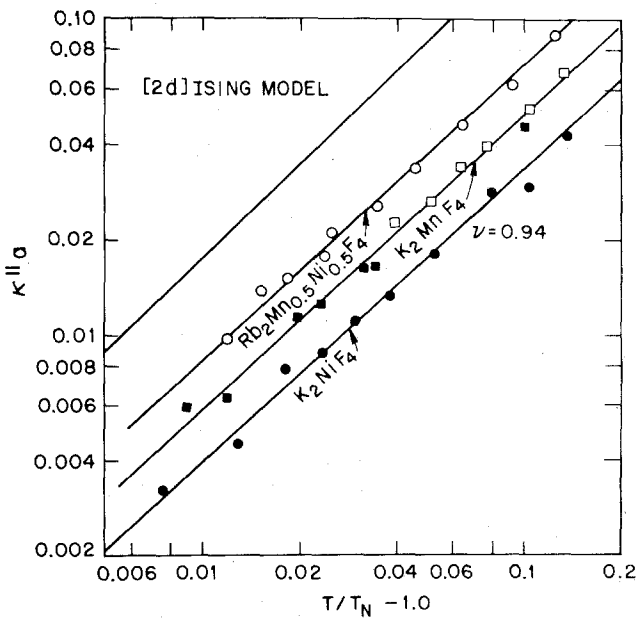

Fig. 2. Inverse correlation lengths for three 2D antiferromagnets together with the exact result for the 2D Ising model. Figure taken from Ref. 3.

$Rb_2Co_cMg_{1-c}F_4$. This system corresponds more closely to an idealized diluted 2D Ising model. He also finds the expected 2D Ising behavior—again without any logarithmic corrections being observable. We have recently confirmed and extended somewhat Ikeda's results in $Rb_2Co_{0.7}Mg_{0.3}F_4$ as part of our general program on random field effects.[9]

Studies of random critical behavior in three dimensions have proven to be surprisingly difficult. Specifically, for a number of years all 3D systems with large randomness seemed to show transitions with pronounced rounding.[10] It was impossible to determine with certainty whether the smearing was due to macroscopic concentration fluctuations or was intrinsic to the physics. Recently, however, this problem has been solved, primarily through an outstanding crystal growth effort at Santa Barbara. V. Jaccarino and co-workers have succeeded in growing high-quality crystals of $Fe_cZn_{1-c}F_2$ and other diluted transition metal fluorides which exhibit phase transitions which are sharp on the 10^{-3} level. This turns out to be

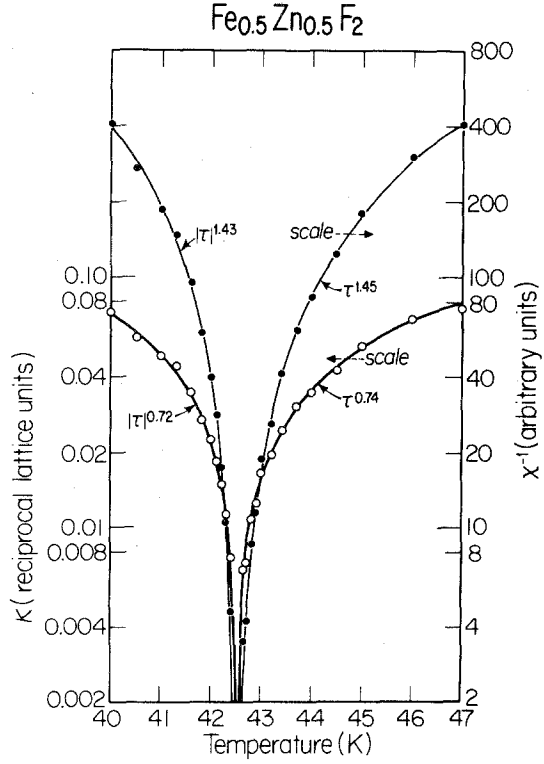

Fig. 3. Inverse correlation length and inverse staggered susceptibility in $Fe_{0.5}Zn_{0.5}F_2$ above and below $T_N = 42.50$ K. The solid lines are the results of fits to single power laws. Figure taken form Ref. 11.

sufficient to observe differences between pure and random Ising critical behavior.[11]

As is by now well known, for 3D n-vector models, only the Ising model which has $\alpha > 0$ is expected to exhibit new critical behavior due to randomness in the exchange.[7] The crossover exponent for the evolution from pure to random critical behavior is $\alpha \simeq 1/9$; thus it was initially expected that the random critical behavior would be unobservable. However, for large randomness with $(\Delta J/J) \sim 1/2$ one has $(\Delta J/J)^{1/\alpha} \simeq 2 \times 10^{-3}$ and the prefactor is unknown; thus the random Ising fixed point could be accessible if the randomness were maximal.

A detailed study of the critical behavior in $Fe_cZn_{1-c}F_2$ with $c = 0.6$ and $c = 0.5$ has been carried out using both birefringence and neutron scattering techniques.[11] FeF_2 has been shown to exhibit 3D Ising critical behavior. The most dramatic effect is observed in the temperature derivative of the birefringence which is proportional to the heat capacity. The measurements show a crossover from divergent behavior with $\alpha = 0.11$ in pure FeF_2 to a cusp with $\alpha = -0.09 \pm 0.03$ in $Fe_{0.6}Zn_{0.4}F_2$. Results for the correlation length and susceptibility in $Fe_{0.5}Zn_{0.5}F_2$ above and below T_N are shown in Fig. 3. First it is found that $\gamma = \gamma'$ and $\nu = \nu'$ to within the errors. Second, as shown in Table I, the results differ considerably from those of the pure 3D Ising model especially for the critical amplitudes. The

Table I. Exponents and Amplitude Ratios for Pure and Random $d = 3$ Ising Models

	Pure Ising		Random Ising	
	Theory[a]	FeF_2[b]	Theory[c]	$Fe_{0.5}Zn_{0.5}F_2$[d]
Susceptibility				
γ	1.24	1.38 ± 0.08	1.39	1.44 ± 0.06
Amplitude ratio	5.1	6.1 ± 1.0	1.7	$2{:}2 \pm 0.1$
Correlation length				
ν	0.63	0.67 ± 0.04	0.70	0.73 ± 0.03
Amplitude ratio	0.53	0.43 ± 0.07	0.83	0.73 ± 0.04
Specific heat				
α	0.11	0.11 ± 0.00	-0.09	-0.09 ± 0.03
Amplitude ratio	0.51	0.54 ± 0.02	-0.5	1.6 ± 0.3

[a] L. C. Guillou and J. Zinn-Justin, *Phys. Rev. B* **21**:3976 (1980).
[b] M. T. Hutchings, M. P. Schulhof, and H. J. Guggenheim, *Phys. Rev. B* **5**:154 (1972); G. Ahlers, A. Kornblit, and M. B. Salamon, *ibid.* **9**:3932 (1974).
[c] Reference 7 and A. Newlove (private communication).
[d] Reference 11.

exponents, however, are in good agreement with recent estimates for those characterizing the 3D random Ising fixed point.[7] We conclude, therefore, that 3D random Ising critical behavior is indeed observable and that recent theory provides reasonable values for the actual exponents. Much better experiments will be required to observe deviations from pure system behavior for the 2D Ising model.

3. PERCOLATION

The essential features of the percolation problem may be seen from Fig. 4. This figure shows a square lattice with 50% of the sites occupied and with only nearest-neighbor atoms connected by bonds. It is evident that for $c = 0.50$ the spins form only finite clusters; in addition, the clusters themselves are highly ramified with many one-dimensional links in the paths between distant atoms on the cluster. If the atoms are decorated with spins with nearest-neighbor exchange interactions, then it is evident that there can be no true phase transition; rather, as $T \to 0$ the correlation length will grow to the size of the large clusters and then saturate.

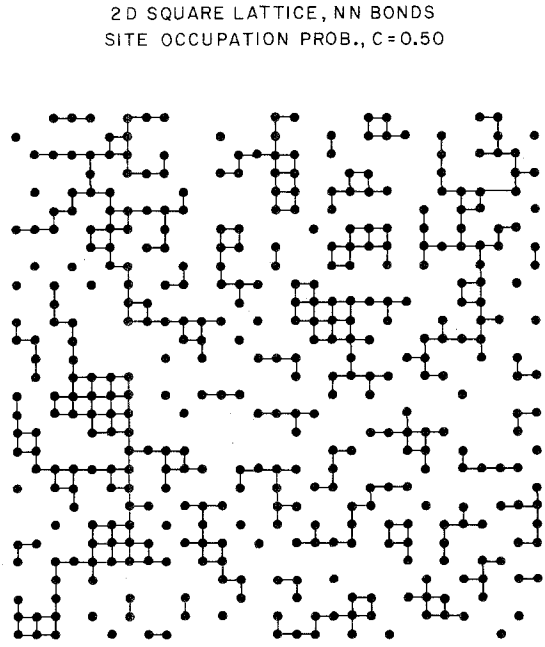

Fig. 4. Computer simulation of a 2D random nn square lattice site percolation network with $c = 0.50$. Only nearest-neighbor bonds are connected. Figure from Ref. 6.

As the concentration is increased the mean size of the clusters, ξ_G, grows until for $c \to c_p$, the percolation concentration, ξ_G diverges and an infinite network is formed. As illustrated in Fig. 1 only for $c \to c_p$ can there be a phase transition at $T > 0$. The behavior around the point ($c = c_p$, $T = 0$) has now been extensively discussed in the literature.[5,6] Briefly, this point may be regarded as a multicritical point exhibiting geometrical critical behavior along the $T = 0$ axis and thermal critical behavior at $c = c_p$ along the temperature axis. The critical exponents are related by the crossover exponent ϕ so that, with an obvious notation, $\gamma_T = \gamma_P/\phi$, $\nu_T = \nu_P/\phi$, etc. The geometrical critical exponents γ_P, ν_P are known quite accurately from various theoretical calculations.[4] The phase boundary for the infinite network for $c > c_p$ is given by $\mu(T_c) \sim (c - c_p)^{\phi}$, where $\mu(T)$ is the appropriate temperature scaling field for the spin system Hamiltonian. As noted previously for Ising models $\mu(T) = 2e^{-2J/kT}$, while for systems with continuous symmetry $\mu(T) \sim T$.

A series of neutron scattering experiments have now been performed in varied one-, two-, and three-dimensional magnets, mapping out the basic behavior around the percolation concentration. As we shall discuss below, these should be regarded as first generation experiments. No attempt was made to explore the subtle line-shape effects which have been the subject of recent theoretical study.[12] We now review the results of these measurements.

3.1. One-Dimensional Magnets

The percolation problem in one dimension is essentially trivial; the percolation concentration in one dimension is, of course, $c_p = 1$ since a single vacancy breaks the chain. The 1D problem, however, turns out to provide useful guidance for the more complicated 2D and 3D systems. For classical unit length spins in 1D one has, as an exact result,[13] the structure factor

$$S(\Delta c, \mu, \mathbf{Q}) \sim \frac{K(\Delta c, 0) + K(0, \mu)}{\left[K(\Delta c, 0) + K(0, \mu)\right]^2 + Q^2} + O\left[(\Delta c)^2, \mu^2\right] \qquad (3)$$

where $K(\Delta c, 0) = 1 - c$ and $K(0, \mu) = \mu = K^{\parallel}_{1D}(T)$. Thus, in 1D the crossover exponent $\phi = 1$.

Experiments have been performed at Brookhaven on the 1D near-Heisenberg magnet $(CD_3)_4NMn_cCu_{1-c}Cl_3$.[14] The Cu–Cu and Cu–Mn interactions are much weaker than the Mn–Mn interactions so that for $k_B T > |J_{Cu-Mn} S_{Cu} S_{Mn}|$ this should simulate the percolation system of interest here. Results for the inverse correlation length K for two samples with $c = 0.85 \pm 0.02$ and 0.93 ± 0.02 by Endoh *et al.*[14] are shown in Fig. 5. The

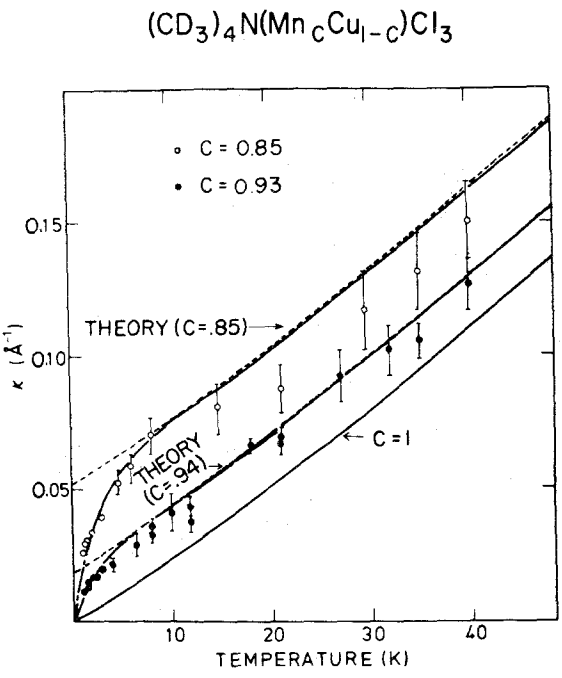

Fig. 5. Inverse correlation length versus temperature in $(CD_3)_4N(Mn_cCu_{1-c})Cl_3$. The dashed lines correspond to the percolation limit with $J_{Mn-Cu} = 0$. The solid lines correspond to the full theory. Figure from Ref. 14, Endoh *et al.*

dashed line represents the results of Eq. (3) with J_{Cu-Mn} set equal to zero and with no adjustment parameters. It is evident that the agreement is quite good, especially for the higher concentration sample provided c is taken as 0.94, which is well within the errors. The departure of the data from the percolation curve for $T \leqslant 8$ K is due to the Cu–Mn coupling; the solid lines are calculated from a theory similar to that given above but including the Cu–Mn interaction.[13]

3.2. Two-Dimensional Magnets

The first experiments in 2D were in the system $Rb_2Mn_cMg_{1-c}F_4$.[6] This is a 2D square lattice with predominantly nearest-neighbor interactions. The spin Hamiltonian for the Mn^{++} may be written

$$\mathscr{H} = \sum_{\langle nn \rangle} J_{nn}\mathbf{S}_i \cdot \mathbf{S}_j - g\mu_B H_A \sum_i (-)^i S_i^z \tag{4}$$

with $J_{nn} \sim 0.72$ meV; the anisotropy field is about 1% of the exchange field.

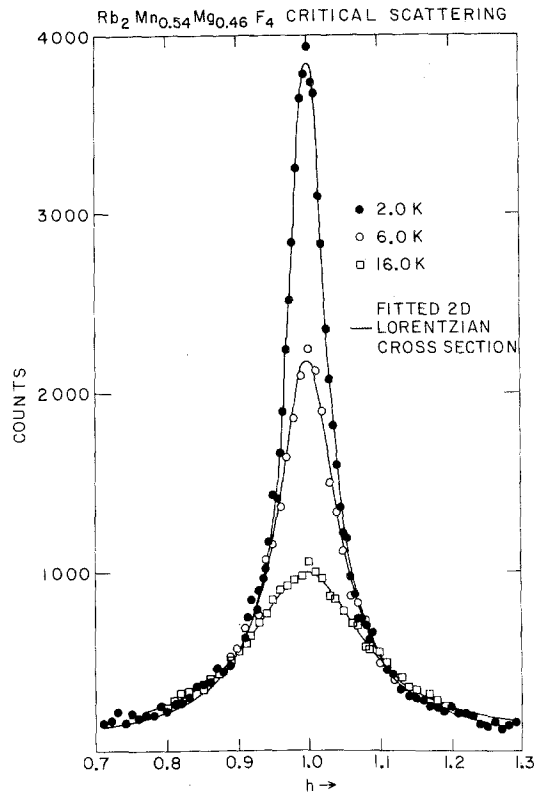

Fig. 6. Critical-scattering scans across the ridge at $(h, 0, 0.4)$ in $Rb_2Mn_{0.54}Mg_{0.46}F_4$ at several temperatures. The horizontal instrumental resolution is $0.011h$, FWHM. The solid lines are the fitted 2D Lorentzians as discussed in the text. Figure from Ref. 6.

This anisotropy term generates some difficulties in the analysis of the experiments; these are discussed in full in Ref. 6; we shall give a simplified discussion of the results here. A series of scans through the antiferromagnetic Bragg peak position in a sample with $c = 0.54$ are shown in Fig. 6. As we noted previously, for the 2D nn square lattice $c_p = 0.594$ so that this sample should be below the percolation threshold. The scattering profiles are well fitted by a simple Lorentzian profile as in 1D. The peak intensity grows and the width narrows as temperature is decreased. However, at $T = 2$ K the width is still much larger than resolution, indicating that the correlation length has saturated at a finite value.

The results for the inverse correlation lengths so obtained are shown in Fig. 7 together with results for samples with $c = 0.57$ and $c = 0.60$. The $c = 0.60$ sample exhibits a phase transition to long-range order at $T \sim 8$ K;

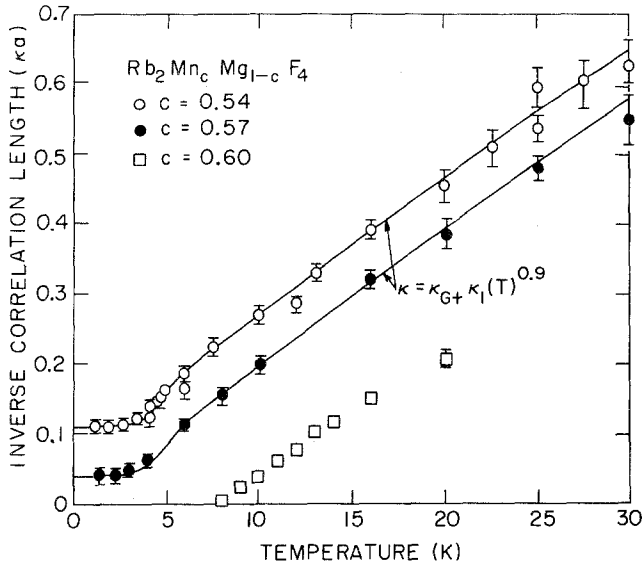

Fig. 7. Fitted inverse correlation lengths vs. temperature in $Rb_2Mn_cMg_{1-c}F_4$ for $c = 0.54$, 0.57, and 0.60. The solid lines represent fits to the percolation multicritical theory as described in text. Figures from Ref. 6.

these results are, of course, in accord with those expected for $c_p = 0.594$. In order to analyze these data quantitatively, it was assumed[6] that the 1D result

$$K(\Delta c, \mu) = K(\Delta c, 0) + K(0, \mu) \tag{5}$$

holds in 2D as well. Further it was argued on heuristic grounds that $\mu = K_{1D}^{\parallel}(T)$ where $K_{1D}^{\parallel}(T)$ is the inverse correlation length of a 1D chain described by the Hamiltonian Eq. (4); this then incorporates the Heisenberg–Ising crossover effects. Fits to this form are shown as the solid lines in Fig. 7. From such fits, one finds $\nu_T = 0.9 \pm 0.1$ and $\gamma_T = 1.5 \pm 0.15$. These may be compared with the 2D percolation exponents $\nu_P = 1.33$ and $\gamma_P = 2.39$; thus for $Rb_2Mn_cMg_{1-c}F_4$ the crossover exponent is $\phi = 1.5 \pm 0.15$. This result was regarded as quite mysterious for a number of years. However, recently Coniglio[15] has succeeded in deriving values for the crossover exponents for systems with continuous symmetry. He has argued that this problem is closely related to the electrical resistance problem on percolating networks. Using available data for the electrical resistance behavior he deduces $\phi = 1.43$ for n-vector models in two dimensions. This agrees within the errors with our experimental value.

An extensive set of experiments have also been performed on the

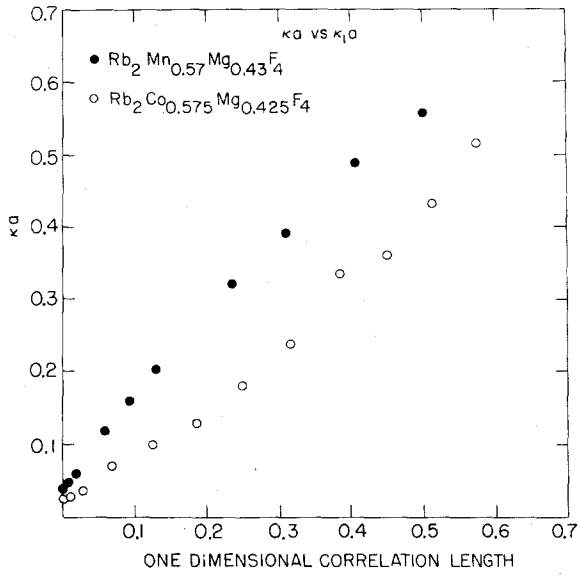

Fig. 8. Measured inverse correlation lengths in $Rb_2Mn_{0.57}Mg_{0.43}F_4$ and $Rb_2Co_{0.575}Mg_{0.425}F_4$ vs. the underlying one-dimensional correlation lengths. For the Mn compound $K_1(T)$ is calculated in Ref. 6 while for the Co compound $K_1(T) = \ln(\tanh \mathcal{J}/kT)$ with $\mathcal{J} = 42$ K. Figure from Ref. 6.

diluted 2D Ising system $Rb_2Co_cMg_{1-c}F_4$.[16] A number of the features observed in $Rb_2Mn_cMg_{1-c}F_4$ hold in the Ising system as well. First, the profiles are again well described by 2D Lorentzians. Second, the sample with $c > 0.594$ exhibits a transition to long-range order while those with $c < 0.594$ exhibit finite correlation lengths at $T = 0$. Third, the fitted inverse correlation lengths are well described as the sums of a geometrical plus a thermal part. Results for a sample with $c = 0.575$ are shown in Fig. 8 together with those from a Mn sample with $c = 0.57$. The results are plotted versus the relevant one-dimensional correlation lengths. It is evident that for $Rb_2Co_cMg_{1-c}F_4$, ν_T must be greater than unity and indeed from detailed fits Cowley *et al.*[16] find $\nu_T = 1.32 \pm 0.04$; they also find, with less certainty, $\gamma_T = 2.4 \pm 0.1$. Using the values given above for the 2D percolation exponents, one deduces a crossover exponent $\phi = 0.99 \pm 0.03$. Wallace and Young[17] have found as an exact result for Ising models in all dimensions $\phi = 1$. Thus, experiment and theory are in excellent accord. Finally we note that, recently, Stinchcombe[18] has provided theoretical arguments for much of the phenomology deduced by us from the analysis of the neutron experiments.

3.3. Three-Dimensional Magnets

Among the most informative experiments were those in the $Mn_cZn_{1-c}F_2$.[19] The Mn^{++} atoms in MnF_2 form a body-centered tetragonal structure with, at low temperatures, the corner Mn^{++} spins oriented along the C-axis antiparallel to the body-center spins. The exhange interactions, which are Heisenberg in character, are predominantly between the corner and body-center spins, although there are also weak interactions between other neighboring pairs.[20] One must also take into account the dipolar coupling which results in a small Ising anisotropy term. Thus, one expects a Heisenberg to Ising crossover in the critical behavior.

Cowley *et al.*[19] employed a novel crystal of $Mn_cZn_{1-c}F_2$ which had a concentration gradient along its length such that it passed through the percolation threshold $c_p = 0.245$ about two-thirds down the crystal. Hence by masking off successive sections it was possible to scan c through c_p. In addition, the geometry of MnF_2 is such that one can measure separately the longitudinal and transverse spin correlation functions. This enabled Cowley *et al.*[19] to observe directly the Heisenberg to Ising crossover. Results for

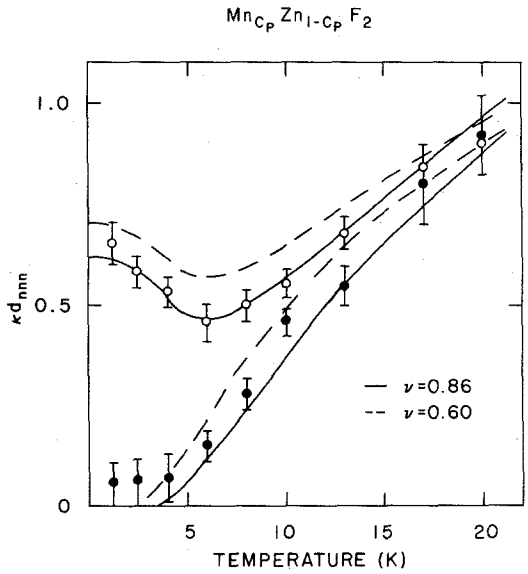

Fig. 9. Transverse (○) and longitudinal (●) inverse correlation lengths vs. temperature in $Mn_{c_p}Zn_{1-c_p}F_2$. The solid lines are calculated using $\nu = 0.86$ ($\phi = 1$) while the dashed lines use $\nu = 0.60$ ($\phi = 1.4$); the latter value was suggested by a model based on a self-avoiding walk approximation to the percolation cluster geometry (Stanley *et al.*, Ref. 5). Figure taken from Ref. 19.

the inverse correlation lengths for $K_{\parallel}$ (closed circles) and $K_{\perp}$ (open circles) are shown in Fig. 9. The solid and dashed lines are calculated assuming $K_{\parallel,\perp} = (K_{1D}^{\parallel,\perp})^{\nu_T}$ with $\nu_T = 0.86$ and $\nu_T = 0.6$, respectively. First, it is evident that the anisotropic behavior in the correlation lengths is very well described by using $K_{1D}^{\parallel,\perp}$ as the temperature scaling field. Second, the exponent $\nu_T = 0.86$ is preferred although the actual value is not known very precisely. Results for a series of concentrations are shown in Fig. 10. The solid lines correspond to the form

$$K_{\parallel,\perp} = K_G + \left(K_{1D}^{\parallel,\perp}\right)^{0.85 \pm 0.10} \tag{6}$$

In 3D, the percolation correlation length exponent is $\nu_P = 0.88 \pm 0.02$. Thus the crossover exponent for $Mn_cZn_{1-c}F_2$ is $\phi = 1.04 \pm 0.14$. This may be compared with the exact result $\phi = 1.0$ for the Ising model and $\phi = 1.12$ for n-vector models. Thus the theories are consistent with experiment although the measurements are not precise enough to distinguish between the discrete and continuous symmetry values for the crossover experiment or a crossover between them.

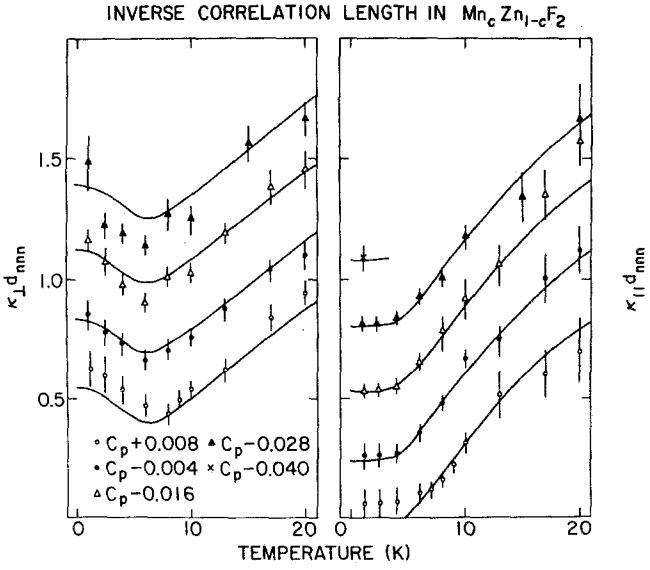

Fig. 10. The inverse correlation length in $Mn_cZn_{1-c}F_2$. Note that in the interest of clarity 0.2 has been added to the results for $c = c_p - 0.004$, 0.4 to $c = c_p - 0.016$, 0.6 to $c = c_p - 0.028$, and 0.8 to $c = c_p - 0.040$. The solid lines are given by $K = (K_G + K_T)$, where K_T is given by the one-dimensional correlation as $K_T a = 0.95\ (K_{1D}a)^{0.85}$ and, for $c < c_p$, $K_G a = 1.3(1 - c/c_p)^{0.845}$ while for $c = c_p + 0.008$, $K_G a = -0.05$, a is the distance between magnetic ions. Figure from Ref. 19.

Detailed results have also been reported for $KMn_cZn_{1-c}F_3$.[19] This is a diluted cubic Heisenberg model with random dipolar anisotropy—a model of considerable current interest. A number of unusual phenomena were observed for c near c_p. Unfortunately, the samples were not of high quality and it was not possible to ascertain unambiguously which effects were intrinsic and which were due, for example, to concentration gradients. The most interesting results were observed for a sample with $c = 0.33$, just above the percolation concentration $c_p = 0.303$. This crystal exhibited a phase transition to long-range order at $T_N \sim 14$ K. However, there was no peak in the critical scattering at T_N and instead the diffuse scattering inverse correlation length, which was nonzero at T_N, decreased gradually to zero as $T \to 0$. In addition, the Bragg scattering reached a maximum at ~ 5 K and then decreased with further decrease in temperature, dropping to a value of about 60% of its peak value. These results have still not been explained satisfactorily. One plausible model is that the diffuse scattering is dominated by the finite clusters while the critical scattering peak at T_N is smeared out by concentration gradients. The diminution of the Bragg intensity would then signify reentrant spin glass behavior driven by a spin glass transition in the finite clusters.[21] We shall discuss this model in more detail in the context of $Eu_cSr_{1-c}S$ in the next subsection.

Finally, we comment that in all of these experiments in 1, 2, and 3D percolative samples, the scattering was Lorentzian in character. However, as discussed in detail by Aharony,[12] at high temperatures the fractal character of the percolation clusters should reflect itself in the line shapes, and deviations from Ornstein–Zernike behavior in the spin–spin correlation function should occur. More detailed experiments at high temperatures are required to test these ideas.

3.4. More Distant Neighbor Interactions

One of the most surprising aspects of all of the results which we have reviewed up to this point is that the experimental percolation threshold corresponds, to within the errors, with that calculated, assuming nearest-neighbor interactions alone. In each case, there are weak (typically 1% to 2%) more distant neighbor exchange couplings as well as long-range dipolar interactions. Although it has not been explicitly proven, we assume that these longer-range interactions do not play a role primarily because of *kinetic* effects. Explicitly, the more distant neighbor couplings do not become comparable in energy with kT until the isolated clusters are frozen. The time to reorient a cluster would then scale like $e^{J_{nn}/kT}$, which may be extremely large at the relevant temperatures.

Very interesting effects, however, may be observed if more distant neighbor interactions are some reasonable fraction of the nn coupling and if they are *competing*, that is, they prefer a different ground state. As demonstrated by Maletta and co-workers,[22] the system $Eu_cSr_{1-c}S$ is a paradigm of such behavior. EuS is a face-centered cubic Heisenberg ferromagnet with $J_{nnn}/J_{nn} = -1/2$. For the fcc lattice[4] $c_p(nn) = 0.195$ while $c_p(nn + nnn) = 0.135$. The experimental phase diagram for the diluted system is shown in Fig. 11. The salient feature is that the ferromagnetism vanishes for $c \simeq 0.51$ rather than 0.195 or 0.135. Between 0.135 and 0.51 a spin glass state occurs at low temperatures. This marked departure from ordinary percolation behavior is explicitly driven by the competition between the nn and nnn interactions. A second novel feature is that, for $c \simeq 0.51$, the ferromagnetism vanishes at low temperatures and a reentrant spin glass is found. This is reminiscent of the behavior in $KMn_cZn_{1-c}F_3$ just above c_p.[19]

Detailed neutron scattering studies have now been carried out on the reentrant spin glass behavior in $Eu_cSr_{1-c}S$. These experiments are discussed in detail in Ref. 22. A number of interesting new effects are observed. We

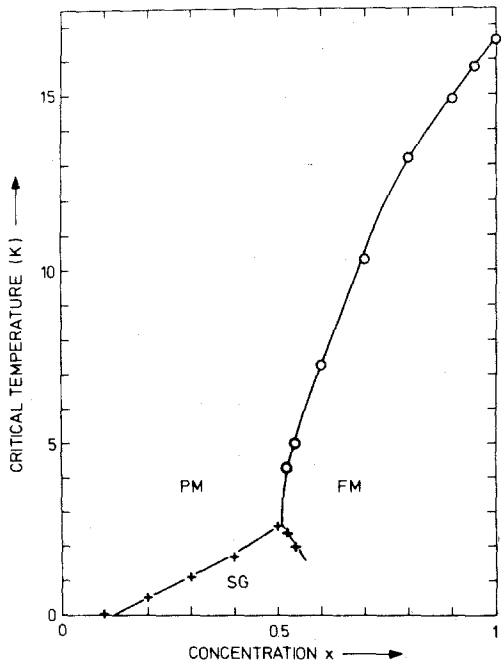

Fig. 11. Experimental phase diagram in $Eu_xSr_{1-x}S$; figure from Ref. 22.

remind the reader that in our percolation experiments the diffuse scattering was always Lorentzian in character. In the reentrant spin glass region it is found that significant deviations from Lorentzian behavior occur. Specifically, $q^{2.6}$ tails are observed. Aeppli *et al.*[19,21] have discussed these effects using a model involving random field coupling between the interpenetrating ferromagnetic and spin glass networks.

4. RANDOM FIELD EFFECTS

In Section 2 it was shown that small randomness in the interaction has at most very subtle effects on the critical behavior. On the other hand random magnetic fields, that is site-random fields with mean value zero but finite variance, are expected to have quite drastic consequences.[23] Specifically, a ferromagnet in $6 - \epsilon$ dimensions with random fields is expected to exhibit the critical behavior of the equivalent pure system in $4 - \epsilon$ dimensions. For systems with continuous symmetry this result is believed to hold down to physically accessible dimensions. This means that the lower critical dimensionality for the random field n-vector model with $n \geqslant 2$ is 4. Thus there should be no phase transition in such systems in three dimensions.

The situation for the Ising model is, however, much more controversial.[24,25] The above $d \to d - 2$ argument would give 3 as the lower critical dimensionality d_l of the random field Ising model. Certain calculations support this result.[24] However, a variety of interface calculations, which are believed to be valid at low temperatures, as well as scaling arguments, yield $d_l = 2$ for the random field Ising model.[25] This would suggest that the 3D random field Ising model should exhibit a phase transition to long-range order (LRO) at some finite temperature. Although random fields are ubiquitous in Nature, initially it seemed quite difficult to carry out systematic experiments on the random field problem. However, Fishman and Aharony[26] pointed out that if a uniform magnetic field is applied to a random Ising antiferromagnet then random staggered magnetic fields would be generated. They further suggested that this system would be isomorphous to the idealized problem of a ferromagnet in a random field. As emphasized by Wong *et al.*,[27] the random staggered field contains a temperature-independent contribution from the randomness in the moment and a temperature-dependent bond randomness term. There are also cross terms between these two effects.[28,29] The Fishman–Aharony suggestion has made possible systematic experimental study of the random field Ising model, albeit in systems which combine random fields and random interactions.

Before discussing individual experimental results, we first state the general situation as of the writing of this paper (September 1983). In all 3D anisotropic systems in which the samples were of high enough quality that

extinction effects could be observed and detailed line-shape analyses could be performed, the LRO was destroyed provided that the quasiordered state was approached from the disordered direction—either by cooling in the field or by fixing the temperature and lowering the field from the paramagnetic state. However, the length scale is quite large. For example in $Fe_{0.6}Zn_{0.4}F_4$ at $H = 20$ kG the correlation length in the quasiordered state is about 1000 lattice constants.[30] This large length scale makes meaningful computer simulations very difficult. A second important feature of the random field problem is that there are remarkable hystereses and long time relaxation effects.[28,30–36] First, even when cooled in a field, 3D systems typically do not respond to changes in the field for $T \lesssim 0.8 T_N$. Thus, the experiments do not access the low-temperature region where the theoretical calculations are expected to be valid[25] or, more correctly, the theories may not be valid in the region where the physical state is established. Second, if the sample is cooled in zero field and a small applied field is switched on, then the LRO state remains stable; indeed the LRO is not destroyed until the sample is heated up to near the "quasiordering" temperature.[30,32] Finally, we note that striking heat capacity effects are observed at small fields where the domain wall separation is very large.[33,34] We now review briefly the published neutron scattering results.

To date neutron scattering experiments have been performed on $Rb_2Co_{0.7}Mg_{0.3}F_4$,[9] $Rb_2Mn_{0.5}Ni_{0.5}F_4$,[35] $Co_cZn_{1-c}F_2$,[28] $Mn_cZn_{1-c}F_2$,[35,36] $Fe_cZn_{1-c}F_2$,[30] $Fe_cMg_{1-c}Cl_2$,[32] $Fe_cCo_{1-c}Cl_2$,[32] and $Dy(P_{0.92}V_{0.08})O_4$.[37] Full papers have been published on the $Rb_2Co_{0.7}Mg_{0.3}F_4$, $Co_cZn_{1-c}F_2$, and $Mn_{0.78}Zn_{0.82}F_2$ neutron scattering experiments while some results on the other systems are available at the time of this writing either in brief preprints or in preliminary reports. The interpretation of these experiments is still evolving. Heat capacity and susceptibility data as a function of applied field are also available for most of the above systems.[33,34,38,39]

An extensive set of experiments have been reported in the diluted 2D Ising antiferromagnet $Rb_2Co_{0.7}Mg_{0.3}F_4$.[9] The essential features are illustrated in Fig. 12 which shows scans through the $(1,0,0)$ magnetic Bragg peak position as a function of decreasing temperature in an applied field of 40 kG. The Néel temperature at $H = 0$ is $T_N = 42.5$ K. The diffuse scattering narrows continuously down to about 20 K and then saturates for lower temperatures. The scattering at 5 K is significantly broader than the resolution of ~ 0.005 Å^{-1} half-width-at-half maximum (HWHM) indicating that the LRO has been destroyed by the applied field. The profile evolves from a Lorentzian at 60 K to a function which can be approximated by a Lorentzian raised to the 3/2 power at 5 K. In fact, theory

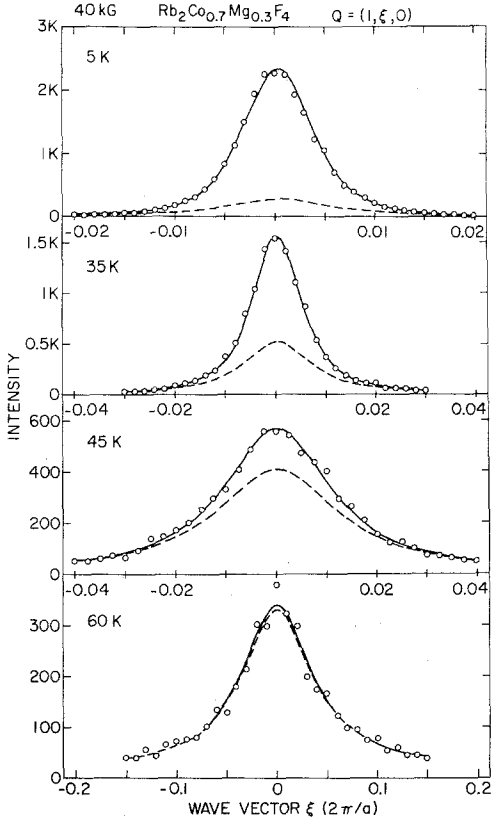

Fig. 12. Quasielastic scattering in $Rb_2Co_{0.7}Mg_{0.3}F_4$ for 40 kG at four different temperatures. Note that the horizontal and vertical axes change between the different temperatures.

suggests as an appropriate form for the structure factor[24]

$$\mathcal{S}(\mathbf{Q}) = \frac{A}{(K^2 + q^2)^2} + \frac{B}{(K^2 + q^2)} \tag{7}$$

where $\mathbf{q} = \mathbf{Q} - \mathbf{G}$. Further, it is argued in Ref. 9 that $A \sim \langle S^z \rangle^2_{H=0} K^{4-d}$ for $T < T_N$ and small H. The solid lines in Fig. 12 represent the results of fits to Eq. (7); the dashed line shows the Lorentzian component.

From a series of such experiments one can extract K vs. H at various temperatures. The results so obtained are shown in Fig. 13. In this 2D system, the equilibration problems are much less severe[9] than those for the 3D systems to be discussed below.[28,30,32] In particular it was explicitly

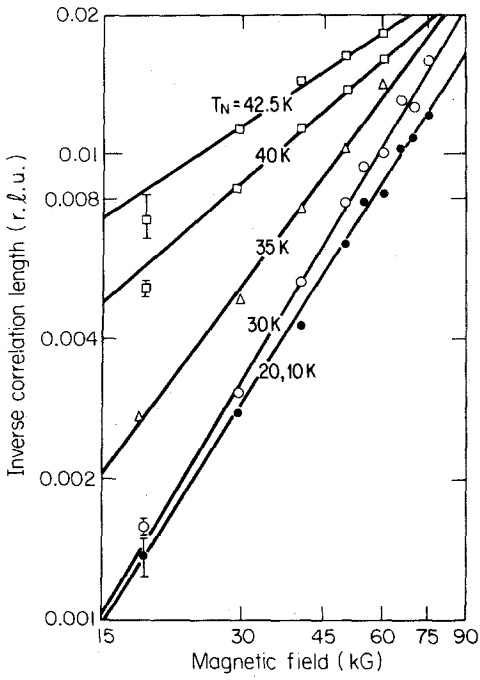

Fig. 13. Logarithmic plot of the fitted inverse correlation length K in $Rb_2Co_{0.7}Mg_{0.3}F_4$ vs. magnetic field at a series of temperatures. The data at 20 K and 10 K are indistinguishable. Figure from Ref. 9.

demonstrated in Ref. 9 that all data down to 30 K and for $H \gtrsim 45$ kG down to 20 K, represent the true equilibrium states. However, at 10 K, $Rb_2Co_{0.7}Mg_{0.3}F_4$ explicitly does not respond to changes in the field and thus must be considered frozen. It is found from the data in Fig. 13 that the exponent $\nu_H(T)$ in

$$K \sim H^{\nu_H(T)} \tag{8}$$

increases gradually from 0.7 ± 0.2 at T_N to 1.6 ± 0.2 at 20 K. The difference between the 30 K and 20 K slopes is not significant. From the scaling theories[25] near T_N one has

$$K(T_N) \sim H_{\mathrm{RF}}^{1.14} \tag{9}$$

while for $T = 0$, theory[23–25] gives for 2D in equilibrium

$$K \sim H_{\mathrm{RF}}^2, \qquad d_l = 3 \tag{10a}$$

or

$$K \sim e^{-C/H_{RF}^2}, \qquad d_l = 2 \tag{10b}$$

Presumably as the temperature is lowered below T_N the exponent should increase continuously from a value of 1.14 to either 2 [Eq. (10a)] or ∞ [Eq. (10b)].

The experiment appears to favor Eq. (10a) and therefore $d_l = 3$ in that the low-temperature exponent $\nu_H = 1.6 \pm 0.2$ is reasonably close to the value 2. The discrepancy at T_N, $\nu_H = 0.7 \pm 0.2$ vs. 1.14 almost certainly originates from the fact that the experiments are not in the small-H limit so that higher-order terms are important. Because of the irreversibility effects at low temperatures the above result is somewhat ambiguous. A theory which predicts the explicit evolution from $T = T_N$ to $T = 0$ is required to choose definitively between the $d_l = 2$ and $d_l = 3$ models.[40] Finally, we note that the experiments give $\mathscr{S}(\mathbf{G}) \sim K^{-2.0}$ in agreement with theory.[9,25] The experiments, of course, also show that the applied field and therefore the induced staggered random field destroy the long-range order. The destruction of the phase transition in $RbCo_cMg_{1-c}F_4$ also manifests itself in the heat capacity and susceptibility behavior. Ferreira *et al.*[39] have shown that the heat capacity for small H near T_N follows quite well the form predicted by random field scaling theory.

The situation in three dimensions is much more complex. Before discussing the neutron scattering experiments we first review the results of heat capacity experiments by the Santa Barbara group[33]; the most precise experiments are in a crystal of $Fe_{0.6}Zn_{0.4}F_2$ which has a very sharp transition at $H = 0$. This is the same crystal which was used for the random Ising critical heat capacity experiment[11] discussed in Section 2. First, it is found for fields up to 20 kG that the heat capacity peak remains sharp; further at both 14.1 and 20 kG, the peak is reasonably well described as a symmetric logarithmic divergence, that is, $\alpha = 0$ over the reduced temperature range $10^{-3} < |T/T_N - 1| < 10^{-2}$. Second, the heat capacity peak temperature follows the Fishman–Aharony[26] crossover form

$$T_c = T_N - bH^2 - cH^{1/\phi} \tag{11}$$

with $\phi = 1.40 \pm 0.05$. According to the scaling theory, the crossover exponent ϕ should equal γ, the susceptibility exponent for the $H = 0$ transition. As shown in Table I, the neutron experiments[11] yield $\gamma = 1.44 \pm 0.06$. This provides very strong evidence that the lowering of T_c is in fact due to the random field mechanism. It should be emphasized, however, that Eq. (11) should hold for a transition either to true LRO or into a quasiordered domain wall state. Belanger *et al.*[33] have argued from the sharpness of the heat capacity peak that they are observing a true phase transition (presum-

ably to antiferromagnetic LRO) and further that the $\alpha = 0$ result reflects 2D Ising behavior. As we shall discuss below, in our view the actual situation is more complex, albeit also more interesting. Specifically, if the crystal is cooled in a field it evolves continuously into a domain wall state.[30] The sharp heat capacity peak then arises from the ordering process within the domain.

Before discussing the neutron results we should also note that there are many other measurements of susceptibilities, heat capacity, etc. in diluted antiferromagnets in a field reported in the literature.[27,34,38] All of these experiments suggest broadened transitions at large H for field-cooled measurements and they have been interpreted as demonstrating the destruction of the phase transition by the induced random fields.

The first published 3D Ising random field neutron scattering experiments[28] were on the system $Co_cZn_{1-c}F_2$ with $c = 0.26$ and 0.35. The results are similar to those in the 2D systems with two important differences. First, as we shall discuss below, in 3D Ising systems the irreversibility effects are much more severe. Second, in $Co_{0.35}Zn_{0.65}F_2$ a novel "relief of extinction" effect is observed at low fields. We first discuss the general behavior. As in 2D, when the $Co_cZn_{1-c}F_2$ samples are cooled in a field

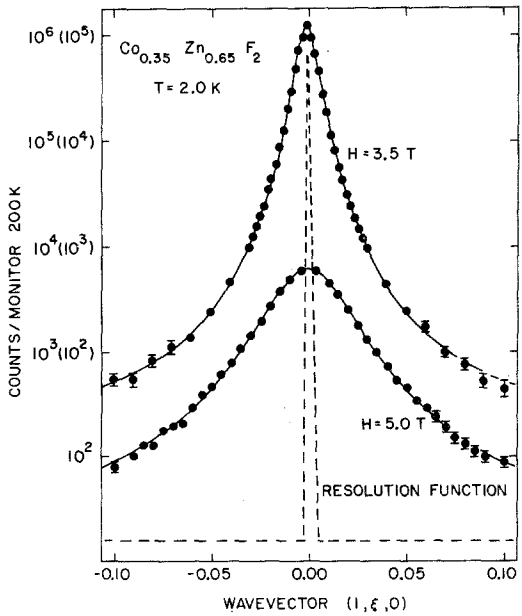

Fig. 14. Scattering for wave-vector transfers along [1ζ0] at 2.0 K from $Co_{0.35}Zn_{0.65}F_2$. The solid lines are fits to Eq. (7) as described in the text. Figure from Ref. 28.

from above T_c, the scattering profiles around the zero-field Bragg position evolve continuously from Lorentzian critical scattering at high temperatures to a Lorentzian-squared profile at low temperatures. We show in Fig. 14 representative results for $Co_{0.35}Zn_{0.65}F_2$, which has $T_N(H = 0) = 13.25$ K, at $T = 2$ K cooled in fields of 35 and 50 kG. Clearly, the line shapes, which are predominantly Lorentzian-squared in form, are much broader than resolution thence demonstrating that the random field has destroyed the LRO. Results of Hagen *et al.*[28] for the temperature dependence of the inverse correlation length K as a function of temperature for a series of fields are shown in Fig. 15. These results are quite similar to those in $Rb_2Co_{0.7}Mg_{0.3}F_4$ shown in Fig. 13. Power law fits to the 2 K data yield $\nu_H = 3.6 \pm 0.3$ and $\mathscr{S}(\mathbf{G}) \sim K^{-3}$ to within the errors. We shall discuss the significance of the power 3.6 ± 0.3 after reviewing the other experiments.

One result in the $Co_{0.35}Zn_{0.65}F_2$ experiment which was initially quite surprising was that at small fields the pseudo-Bragg peak intensity in-

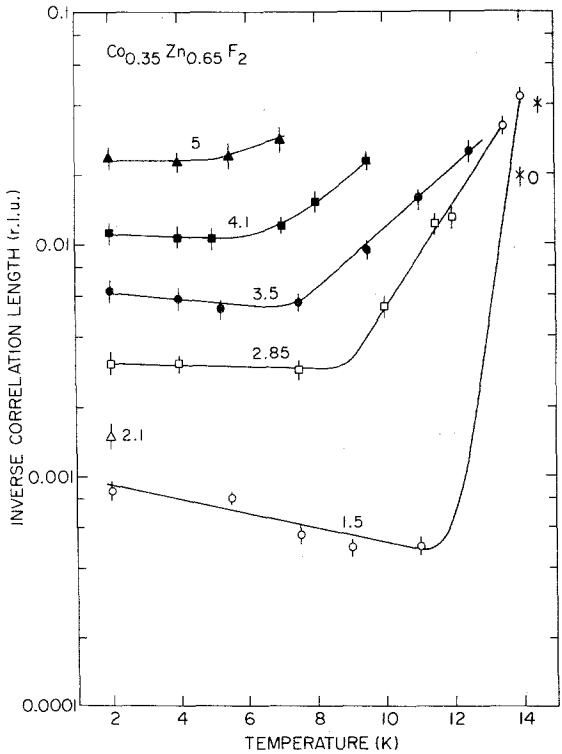

Fig. 15. Inverse correlation length K deduced for $Co_{0.35}Zn_{0.65}F_2$ as a function of temperature for various applied fields. Figure from Ref. 28.

creased with increasing field.[28] This is the exact opposite of what one would naively expect if the field destroyed the LRO. Comparison with nuclear peaks showed that only the magnetic peaks exhibited this effect. Hagen *et al.*[28] explain this anomalous increase by considering the effects of extinction. In zero field, the crystal is sufficiently perfect that the magnetic Bragg reflection is *extinction limited*, that is, only that part of the incident beam which satisfies the Bragg condition perfectly is reflected. When the sample is cooled in an applied field, the magnetic order within the mosaic blocks is broken up into domains by the random field effect, and as a consequence the effective Darwin width is increased so that a greater proportion of the incident beam is scattered. Once the inverse width of the domains becomes comparable to the resolution this effect disappears and the peak intensity decreases with further increase in field. Thus in perfect crystals, this effect allows one to see the destruction of LRO by the random fields on length scales much larger than the spectrometer resolution would normally allow. It should also be noted that even when the peaks are resolution-limited, which typically means that the domain wall separation is larger than $\sim$500 lattice constants, one can see the appearance of Q^{-4} tails in the scattering profiles in Ising systems. Since the tail amplitude scales like K in three dimensions this enables one to connect continuously onto the region where K is directly measurable.

Experiments have also been performed on $Mn_cZn_{1-c}F_2$ with $c = 0.78$[36] and $c = 0.65$.[35] As discussed in Section 3, MnF_2 is a body-centered tetragonal antiferromagnet with Heisenberg exchange interactions and a small Ising anisotropy due to the dipolar interactions.[20] Thus it should show 3D Ising random field behavior. Initial bulk experiments[33,34] showed that T_c was reduced by the applied field according to Eq. (11) with $\phi = 1.1$ to 1.4, thence verifying the importance of the random field effects. Shapira *et al.*[34] and Ikeda *et al.*[38] both showed that the transition was broadened at large fields and they interpreted this as the destruction of the phase transition by the random field. This interpretation has been criticized by Belanger *et al.*,[33] who suggest that the broadening instead may reflect the proximity of the bicritical point which is Heisenberg in character. In our view this criticism is inappropriate, since only *randomly oriented* random fields will destroy the phase transition in a 3D Heisenberg system; a uniaxial random field simply favors a LRO phase with the spins oriented perpendicular to the random field direction. This conclusion could be modified by off-diagonal coupling terms of the form $S^{\parallel}S^{\perp}$. However, since Mn^{++} is an S-state ion, these effects will be totally negligible.

Initially neutron experiments[36] on $Mn_{0.78}Zn_{0.22}F_2$ were interpreted as implying that the LRO was *not* destroyed by the random field at least on the length scale of 1200 lattice spacings. More recent experiments by the

authors together with the Santa Barbara group[35] on $Mn_{0.65}Zn_{0.35}F_2$ were also initially interpreted by us[41] as implying LRO at low temperatures for all fields. More careful examination in the light of recent results in $Fe_cZn_{1-c}F_2$ shows that this is not the case. First, in $Mn_{0.78}Zn_{0.22}F_2$, Cowley and Buyers[36] found that the scattering around T_c (47.0 to 48.0 K) for $H = 40$ kG was indicative of Lorentzian plus Lorentzian-squared behavior as found in $Co_cZn_{1-c}F_2$. However, for $T < 47.0$ K the profiles were resolution-limited, as also found in $Co_cZn_{1-c}F_2$ at small fields. For the configuration used by Cowley and Buyers,[36] this implies $K < 0.0017$ Å^{-1} or $\xi = K^{-1} > 350$ lattice constants (there is an error by $\sim\pi$ in the published estimate of 1200 quoted above). From more recent data, it is possible to put these results on an absolute scale in H/J. Specifically, a simple scaling as a function of concentration from the results in the $Fe_cZn_{1-c}F_2$ series to be discussed below shows that for $c = 0.78$ and $H = 40$ kG, the domain wall separation should indeed exceed 350 lattice constants. Thus the experiments cannot be interpreted as implying that $Mn_cZn_{1-c}F_2$ differs from the good Ising systems. This again illustrates the importance of appropriate consideration of the relevant length scales in these random field problems. The more recent experiments[35] on $Mn_{0.65}Zn_{0.35}F_2$, which are not yet published, show each of (i) a pronounced rounding of the transition, (ii) the relief-of-extinction effect, and (iii) Lorentzian plus Lorentzian-squared profiles down to 7 K when the sample is cooled in a field. Again the length scales are quite large, albeit not qualitatively different from those found in $Fe_{0.6}Zn_{0.4}F_2$. Thus the results in $Mn_cZn_{1-c}F_2$ are similar to those in the good Ising systems and they exhibit the destruction of LRO in field-cooled samples by the random field.

The most complete experiments have been performed on the system $Fe_cZn_{1-c}F_2$ discussed in Section 2. As noted previously, very high quality crystals have been grown at Santa Barbara[33] with $c = 0.35$, 0.50, and 0.60. The data from the neutron scattering experiments using these samples are still being analyzed so that we cannot give a proper description of the measurements here. In general, however, the results are similar to those discussed above for $Co_{0.35}Zn_{0.65}F_2$, albeit rather more thorough. In all three crystals it has been shown that for all fields the field-cooled transition is into a Lorentzian-squared state; at small fields the length scale is quite large so that the effects of the random fields are seen through the relief of extinction and the Q^{-4} tails in the resolution-limited scattering profiles. Again, relaxation and irreversibility effects play a dominant role. Reproducible results down to $\sim 0.8T_c$ are obtained if the state is approached from the disordered direction. However, if the state is approached from a more ordered direction, for example, by cooling below T_N in zero field and then turning on the field, one only recovers the Lorentzian-squared state if

the sample is warmed to near T_c. The fact that for intermediate temperatures the K characterizing the Lorentzian squared state decreases with decreasing H but remains fixed on the time scale of minutes to hours if H is then increased, suggests that the irreversibility effects originate in the difficulty in nucleating domain walls. Similar behavior has been seen in temperature cycling of commensurate–incommensurate transitions.[42] In $Fe_cZn_{1-c}F_2$ the state is completely frozen for $T \lesssim 0.8T_c$. Thus all of the measurements must be regarded as reflecting the high-temperature behavior. The experiments may not probe the true low-temperature equilibrium state. However, since in nearly all physical realizations of random fields in Nature, the random fields are present at high temperatures, it is the field-cooled behavior which must be understood.

In the Lorentzian-squared region in $Fe_cZn_{1-c}F_2$ the neutron experiments reveal that $\nu_H = 2.1 \pm 0.1$ and for the 35% sample at least, this power law holds for $\xi = K^{-1}$ varying from $\sim$15 Å to at least 1500 Å; it is also found that $\mathscr{S}(\mathbf{G}) \sim K^{-3}$ as expected. As noted above, these power laws must be regarded as reflecting the *high-temperature* field cooled behavior since the state is frozen below $\sim 0.8T_c$. This presumably accounts for the differences in the exponents in $Co_cZn_{1-c}F_2$ and $Fe_cZn_{1-c}F_2$. As we noted previously, the length scales for $Fe_{0.6}Zn_{0.4}F_2$ for fields of 14.1 and 20 kG are about 2000 and 1000 lattice constants, respectively. Thus, it is not surprising that Belanger *et al.*[33] observe sharp peaks in the heat capacity at the 10^{-3} level. The crossover to $\alpha \sim 0$ is, however, a surprising and important feature which, in our view, remains to be understood within the context of the overall behavior revealed by the neutron experiments. Interesting fluctuation effect are also found in the neutron experiments[30] in this field-temperature range in $Fe_{0.6}Zn_{0.4}F_2$; these data are still being analyzed so that we cannot present the final empirical picture here.

It is clear, however, that in the view being presented in this paper, the heat capacity singularity must ultimately become rounded when the length scale for the fluctuations producing the heat capacity peak becomes comparable with the domain wall separation. High-precision data at high fields in $Fe_{0.6}Zn_{0.4}F_2$ are not yet available. However, Shapira *et al.*[34] have measured the thermal expansion in $Mn_{0.75}Zn_{0.25}F_2$ up to the bicritical point. In equilibrium, the thermal expansion exhibits the critical behavior of the heat capacity. At low fields, for field-cooled samples they observe a sharp heat capacity peak which is more symmetric than at $H = 0$, in agreement with the $Fe_{0.6}Zn_{0.4}F_2$ results. However, at larger fields this peak broadens considerably and the phase transition is clearly destroyed. In addition, Shapira *et al.* find that (i) hysteresis effects are seen for $H \geqslant 20$ kOe; (ii) the peaks are sharper when warming, after cooling at the same H, and sharpest when warming after cooling at zero field. These features agree with our neutron

results in $Mn_{0.65}Zn_{0.35}F_2$. We believe, therefore, that there is no disagreement at all between the experimental neutron and heat capacity results. The only possible differences are in the interpretation of the measurements. Of course, as we stated above, the crossover of the heat capacity to a symmetric logarithmic peak at low fields remains to be understood.

Before giving our overall view of the random field problem we briefly discuss experiments in other systems. Wong and Cable[32] have carried out experiments on $Fe_cMg_{1-c}Cl_2$ and $Fe_cCo_{1-c}Cl_2$. The former gives results similar to those in the diluted fluorides, especially insofar as the irreversibility effects are concerned. The latter is a complicated system with competing anisotropies.[43] Wong and Cable[32] have studied a sample $Fe_{0.275}Co_{0.725}Cl_2$ in a magnetic field. In *zero* field this sample[43] exhibits successive Ising and 3-component Potts transitions[44] with decreasing temperature. The latter transition is rounded due to random field effects originating from random coupling terms between the longitudinal and transverse spin components. On application of a small field, Wong and Cable find that the profiles of the Ising component below T_N are always resolution limited. However, since their resolution is four times worse than that used in our experiments, it is not clear how much significance one should assign to this latter result. The most interesting measurements in the above crystal are in the spin-flop phase. This should be a realization of the three-component Potts model in a random field. Wong and Cable[32] indeed are able to see the destruction of LRO. Unfortunately, the samples are of too poor quality to allow the kind of detailed line-shape analysis possible in the fluorides. Kettler and Steiner[37] have studied the random field behavior in $Dy(P_{0.92}V_{0.08})O_4$. This is a 3D Ising antiferromagnet with the Ising anisotropy partially random in magnitude and direction.[45] At $H = 0$ it exhibits a sharp Ising transition to LRO. When the system is cooled in a field, the LRO is destroyed as in our diluted fluoride experiments. Irreversibility effects are also observed. The experiments on this system are still in progress so that complete results including, especially, detailed line-shape analyses are not yet available. The initial results themselves are, nevertheless, quite important since they show that the destruction of LRO in 3D Ising magnets by random fields is not just a property of *diluted* magnets but instead is a more general feature.

Suter *et al.*[46] have used high-resolution x-ray scattering techniques to study the Ag ordering in $TiS_2Ag_{0.33}$. This is believed to be a realization of the 3D XY model with sixfold anisotropy. Impurities in this system generate site-random pinning fields. Because of the discrete nature of the anisotropy, Suter *et al.*[46] expect this system to exhibit behavior analogous to that of the 3D Ising model in a random field. They find that the low-temperature state does not have LRO but rather the profiles are

well-described by the Lorentzian-squared line shape, albeit with a large domain size. The phase transition is also rounded.

Random field effects are important in a wide variety of other magnetic systems. Birgeneau and Berker[47] have discussed the effects of impurities on metamagnetic tricritical point measurements. Because such tricritical points involve the application of a bulk magnetic field there are then induced random fields acting on both the magnetization and the sublattice magnetization. By a careful consideration of the crossover effects, Birgeneau and Berker[47] have shown that many apparently anomalous results in the literature are naturally explained by random fields. Such effects may be important in other multicritical point experiments including, especially, bicritical measurements like those in $Mn_cZn_{1-c}F_2$ and $Gd_cLa_{1-c}Al\,O_3$.[48] As we noted above, Wong *et al.*[43] have pointed out in random alloys with competing spin anisotropies such as $Fe_cCo_{1-c}Cl_2$, the achievement of LRO in one order parameter will generate random fields on the order parameter through the off-diagonal coupling. This has a profound effect on the multicritical phase diagram. Such effects are seen in the $Fe_cCo_{1-c}Cl_2$ experiments. As we already discussed in Section 3, in systems with competing ferromagnetic and antiferromagnetic interactions there is a crossover from from ferromagnetism to spin-glass behavior. For concentrations near this crossover point, the ferromagnetic order vanishes at low temperatures. Aeppli *et al.*[21] have modeled such systems as interpenetrating spin-glass and ferromagnetic networks. They have then pointed out that if the spin-glass network undergoes a transition at low temperatures it will set up quenched random fields on the ferromagnetic system. This in turn will cause the ferromagnet to break up into microdomains. Many of the features of reentrant spin-glass systems, especially the neutron scattering results, are simply explained using this model.

It is clear, therefore, that random fields have profound effects on the properties of magnets in both two and three dimensions. It is equally clear, however, that we do not have a proper theoretical understanding of these effects. Manifestly, irreversibility plays a dominant role. Many theories now predict that 3D random field Ising magnets should exhibit LRO at low temperatures provided that the equilibrium state is accessible.[25] As we have discussed in this paper, in all cases in which it is possible to carry out high-resolution measurements it has been found that for systems cooled in the presence of the random fields, the phase transition is destroyed and one instead freezes continuously into a "Lorentzian-squared" disordered state. As we have stressed in this paper, the length scale for this disordered state may be quite large. All of the physical realizations of the random field Ising model involve a combination of random fields and random interactions. It

is not yet certain how important this combined randomness is, although our prejudice is that the physics is dominated by the random field component. The irreversibility and long relaxation time phenomena are, however, clearly of profound significance. In order to make progress on the theoretical front, these effects will have to be taken into account explicitly. For additional comments on the theoretical issues as well as a general review of the theory, the reader should see the paper by Imry[49] in this issue.

ACKNOWLEDGMENTS

We should like to acknowledge pleasant and stimulating interactions with our collaborators J. Als-Nielsen, D. P. Belanger, A. N. Berker, M. Hagen, H. J. Guggenheim, H. Ikeda, V. Jaccarino, A. R. King, S. K. Satija, E. C. Svenssen, and J. A. Tarvin. We have benefited greatly from discussions with G. Aeppli, A. Aharony, J. L. Cardy, D. S. Fisher, P. M. Horn, G. Grinstein, Y. Imry, P. A. Lee, T. C. Lubensky, D. Mukamel, E. Pytte, Y. Shapira, H. E. Stanley, M. Steiner, D. J. Wallace, and P. Wong. We should also like to thank V. Jaccarino, Y. Shapira, M. Steiner, and P. Wong for communicating their results prior to publication. The work at Brookhaven National Laboratory was supported by the Division of Basic Energy Sciences, U.S. Department of Energy, under Contract No. DE-AC0276CH0016; the work at Massachusetts Institute of Technology was supported by the National Science Foundation Low Temperature Physics Program under contract No. DMR-79-23203; and the work at Edinburgh was supported by the Science and Engineering Research Council.

NOTE ADDED IN PROOF

Since this manuscript was completed, two important developments have occurred in the random field Ising problem. First, Belanger *et al.*[30] have completed their analysis of the critical scattering data in the $Fe_{0.6}Zn_{0.4}F_2$ system. As we noted in the text, the field-cooled behavior is identical to that observed previously[41] in $Fe_xZn_{1-x}F_2$ with $x = 0.35$ and 0.50. Specifically, it is found that the inverse domain size $K \sim H^2$; further, the absolute magnitude seems to scale reasonably with concentration. At $H = 2.0T$ the field cooled K is of the order of 0.0002 reciprocal lattice units (rlu). Thus, a study of the critical behavior for $0.001 < K < 0.01$ rlu is possible. It is found that the critical scattering is well described by Eq. (7) with the Lorentzian squared term dominant. According to Mukamel and Pytte,[24] in the critical region in Eq. (7) one expects $A/K^4 \sim (T -$

$T_N)^{-\nu(4-\eta)}$ and $B/K^2 \sim (T - T_N)^{-\gamma}$. Belanger *et al.*[30] thence find $\nu = 1.0 \pm 0.1$, $\gamma = 1.8 \pm 0.2$, and $\nu(4 - \eta) = 4.0 \pm 0.4$; these may be combined with the birefringence result $\alpha = 0.00 \pm 0.04$. The corresponding exponents for the 2D Ising model are $\nu = 1.0$, $\gamma = 1.75$, $\nu(4 - \eta) = 3.75$ and $\alpha = 0$. The agreement clearly is very good. Thus it appears that the 3D random field Ising model exhibits 2D Ising equilibrium critical fluctuations in spite of the fact that the field cooled transition is into a domain state.

Stimulated by the experiments described in this review, J. Villain and, independently, G. Grinstein and J. Fernandez have proposed an interesting solution to this problem. R. Bruinsma and G. Aeppli have produced a similar, but not identical, theory. They predict that $d_l = 2$ in equilibrium thus allowing, although not predicting, 2D Ising-like fluctuations for the 3D random field Ising model. However, Villain finds that for samples quenched to a temperature T below the phase boundary the domains are pinned at a critical radius $R_c = Jk_B T H_{rf}^{-2} \ln(t/\tau)$ where τ is a microscopic time constant. Grinstein and Fernandez obtain the same result except for a prefactor of 2. This result holds in both 2 and 3 dimensions. The consequent H_{rf}^{-2} scaling for K describes the results in $Rb_2Co_{0.7}Mg_{0.3}F_4$, $Co_{0.26}Zn_{0.74}F_2$, and the $Fe_xZn_{1-x}F_2$ samples to within the combined uncertainties. It disagrees somewhat with the $H^{3.6\pm0.4}$ behavior found in $Co_{0.35}Zn_{0.65}F_2$. The order of magnitude for R_c turns out to be correct for all of the samples. Finally, the hysteresis is sensibly explained by this critical size pinning mechanism. We note that for τ^{-1} taken as the exchange frequency the domain size changes by less than a factor of 2 for time varying between one hour and the current age of the universe. Thus the LRO is destroyed on all practical time scales. These new theories are clearly very promising although explicit predictions for samples cooled slowly in a field are required before one can be certain that the theories are correct.

REFERENCES

1. R. J. Birgeneau, R. A. Cowley, G. Shirane, J. A. Tarvin, and H. J. Guggenheim, *Phys. Rev. B* **21**:317 (1980).
2. H. Ikeda and K. Hirakawa, *Solid State Commun.* **14**:529 (1974).
3. J. Als-Nielsen, R. J. Birgeneau, H. J. Guggenheim, and G. Shirane, *J. Phys. C* **9**:L121 (1976).
4. See for example, J. W. Essam, in *Phase Transitions and Critical Phenomena*, C. Domb and M. S. Green, eds. (Academic, New York, 1972), Vol. II, p. 197; D. Stauffer, *Phys. Rep.* **54**:1 (1979).
5. D. Stauffer, *Z. Phys. B* **22**:161 (1976); H. E. Stanley, R. J. Birgeneau, P. J. Reynolds, and J. F. Nicoll, *J. Phys. C* **9**:L553 (1976); T. C. Lubensky, *Phys. Rev. B* **15**:311 (1977).
6. R. J. Birgeneau, R. A. Cowley, G. Shirane, J. A. Tarvin, and H. J. Guggenheim, *Phys. Rev. B* **21**:317 (1980).
7. A. B. Harris, *J. Phys. C* **7**:1671 (1974); A. B. Harris and T. C. Lubensky, *Phys. Rev. Lett.* **33**:1540 (1974); T. C. Lubensky, *Phys. Rev. B* **11**:3580 (1975); G. Grinstein and A. Luther,

ibid. **13**:1329 (1976); D. E. Khmel'nitskii, *Zh. Eksp. Teor. Fiz.* **68**:1960 (1975) [*Sov. Phys.-JETP* **41**:981 (1976)]; C. Jayaprakash and H. J. Katz, *Phys. Rev. B* **16**:3987 (1977); K. E. Newman and E. K. Riedel, *Phys. Rev. B* **25**:264 (1982); Giancarlo Jug, *ibid.* **27**:609 (1983); V. Dotsenko and V. Dotsenko, *Adv. Phys.* **32**:129 (1983).

8. H. Ikeda, *J. Phys. Soc. Jpn.* **50**:3215 (1981).
9. R. J. Birgeneau, H. Yoshizawa, R. A. Cowley, G. Shirane, and H. Ikeda, *Phys. Rev. B* **28**:1438 (1983).
10. G. M. Meyer and O. W. Dietrich, *J. Phys. C* **11**:1451 (1978); R. A. Cowley and K. Carneiro, *ibid.* **13**:3281 (1980).
11. R. J. Birgeneau, R. A. Cowley, G. Shirane, H. Yoshizawa, D. P. Belanger, A. R. King, and V. Jaccarino, *Phys. Rev. B* **27**:6747 (1983).
12. For a review see A. Aharony, in *Multicritical Phenomena*, R. Pynn, ed. (Plenum, New York, 1984).
13. M. Thorpe, *J. Phys. (Paris)* **36**:117 (1975).
14. Y. Endoh, G. Shirane, R. J. Birgeneau, and Y. Ajiro, *Phys. Rev. B* **19**:1476 (1979); J. P. Boucher, C. Dupas, W. Fitzgerald, K. Knorr, and J. P. Renard, *J. Phys. (Paris)* **39**:L-86 (1978).
15. A. Coniglio, *Phys. Rev. Lett.* **46**:250 (1981).
16. R. A. Cowley, R. J. Birgeneau, G. Shirane, H. J. Guggenheim, and H. Ikeda, *Phys. Rev. B* **21**:4038 (1980).
17. D. J. Wallace and A. P. Young, *Phys. Rev. B* **17**:2384 (1978).
18. R. B. Stinchcombe, *J. Phys. C* **13**:3723 (1980).
19. R. A. Cowley, G. Shirane, R. J. Birgeneau, E. C. Svennson, and H. J. Guggenheim, *Phys. Rev. Lett.* **39**:894 (1977); *Phys. Rev. B* **22**:4412 (1980).
20. O. Nikotin, P. A. Lingard, and O. W. Dietrich, *J. Phys. C* **2**:1168 (1969).
21. G. Aeppli, S. M. Shapiro, R. J. Birgeneau, and H. S. Chen, *Phys. Rev. B* **25**:4882 (1982); *B* **28**:5160 (1983).
22. H. Maletta and P. Convent, *Phys. Rev. Lett.* **42**:108 (1979); H. Maletta and W. Felsch, *Z. Phys. B* **37**:55 (1980); H. Maletta, G. Aeppli, and S. M. Shapiro, *Phys. Rev. Lett.* **48**:1490 (1982); *J. Magn. Magn. Mat.* **31–34**:1367 (1983).
23. Y. Imry and S-k. Ma, *Phys. Rev. Lett.* **35**:1399 (1975); A. Aharony, Y. Imry, and S-k. Ma, *Phys. Rev. Lett.* **37**:1367 (1976); G. Grinstein, *ibid.* **37**:944 (1976); A. P. Young, *J. Phys. C* **10**:L257 (1977); G. Parisi and N. Sourlas, *Phys. Rev. Lett.* **43**:744 (1979).
24. E. Pytte, Y. Imry, and D. Mukamel, *Phys. Rev. Lett.* **46**:1173 (1981); K. Binder, Y. Imry, and E. Pytte, *Phys. Rev. B* **24**:6736 (1981); D. Mukamel and E. Pytte, *ibid.* **25**:4779 (1982); H. S. Kogon and D. J. Wallace, *J. Phys. A* **14**:L527 (1981); J. Cardy (unpublished); A. Niemi, *Phys. Rev. Lett.* **49**:1808 (1982).
25. G. Grinstein and S-k. Ma, *Phys. Rev. Lett.* **49**:685 (1982); J. Villain, *J. Phys. (Paris)* **43**:L551 (1982); A. Aharony and E. Pytte, *Phys. Rev. B* **27**:5872 (1983).
26. S. Fishman and A. Aharony, *J. Phys. C* **12**:L729 (1979).
27. P. Wong, S. von Molnar, and P. Dimon, *J. Appl. Phys.* **53**:7954 (1982).
28. M. Hagen, R. A. Cowley, S. K. Satija, H. Yoshizawa, G. Shirane, R. J. Birgeneau, and H. J. Guggenheim, *Phys. Rev. B* **28**:2602 (1983).
29. J. Cardy, *Phys. Rev. B* **29**:505 (1984).
30. D. P. Belanger, H. Yoshizawa, V. Jaccarino, A. R. King, R. J. Birgeneau, R. A. Cowley, and G. Shirane (unpublished work).
31. H. Yoshizawa, R. A. Cowley, G. Shirane, R. J. Birgeneau, H. J. Guggenheim, and H. Ikeda, *Phys. Rev. Lett.* **48**:438 (1982).
32. P. Wong and J. Cable, *Phys. Rev. B* **28**:5361 (1983) and unpublished work.
33. D. P. Belanger, A. R. King, and V. Jaccarino, *Phys. Rev. Lett* **48**:1050 (1982); D. P. Belanger, A. R. King, V. Jaccarino, and J. L. Cardy, *Phys. Rev. B* **29**:2522 (1983).

34. Y. Shapira, *J. Appl. Phys.* **53**:1931 (1982); and private communication; Y. Shapira and N. F. Oliveira Jr., *Phys. Rev. B* **27**:4336 (1983); Y. Shapira, N. F. Oliviera Jr., and S. Foner (unpublished).
35. R. A. Cowley, H. Yoshizawa, G. Shirane, R. J. Birgeneau, M. Hagen, and D. P. Belanger (unpublished work).
36. R. A. Cowley and W. J. L. Buyers, *J. Phys. C* **15**:L1209 (1983).
37. P. Kettler and M. Steiner (private communication).
38. H. Ikeda, *J. Phys. C* **16**:L21 (1983); H. Ikeda and K. Kikuta, *ibid.* **16**:L445 (1983).
39. I. B. Ferreira, A. R. King, V. Jaccarino, H. J. Guggenheim, and J. L. Cardy, *Phys. Rev. B* **28**:5192 (1983).
40. E. Pytte (private communication) is currently carrying out such calculations.
41. R. A. Cowley, R. J. Birgeneau, G. Shirane, and H. Yoshizawa, *Proceedings of the Geilo Conference on Multicritical Phenomena*, R. Pynn, ed. (in press) (Plenum, New York, 1984).
42. R. M. Fleming, D. E. Moncton, D. B. McWhan, and F. J. DiSalvo, *Phys. Rev. Lett.* **45**:576 (1980); C. H. Chen, J. M. Gibson, and R. M. Fleming, *Phys. Rev. B* **26**:184 (1982).
43. P. Wong, P. M. Horn, R. J. Birgeneau, and G. Shirane, *Phys. Rev. B* **27**:428 (1983).
44. A. N. Bazhan and V. A. Ul'ganov, *Zh. Eksp. Teor. Fiz.* **79**:186 (1980) [*Sov. Phys.-JETP* **52**:94 (1980)]; D. Mukamel, *Phys. Rev. Lett.* **46**:845 (1981).
45. P. Kettler, M. Steiner, H. Dachs, R. German, and B. Wanklyn, *Phys. Rev. Lett.* **47**:1329 (1981).
46. R. M. Suter, M. W. Schafer, and P. M. Horn, *Phys. Rev. B* **26**:1495 (1982).
47. R. J. Birgeneau and A. N. Berker, *Phys. Rev. B* **26**:3751 (1982).
48. H. Rohrer and H. J. Scheel, *Phys. Rev. Lett.* **44**:876 (1980). In this paper it is shown that random fields round the Ising transition as we expect.
49. Y. Imry, this issue, *J. Stat. Phys.* **34**:849 (1984).